

# Monolayer Graphene/Germanium Schottky Junction As High-Performance Self-Driven Infrared Light Photodetector

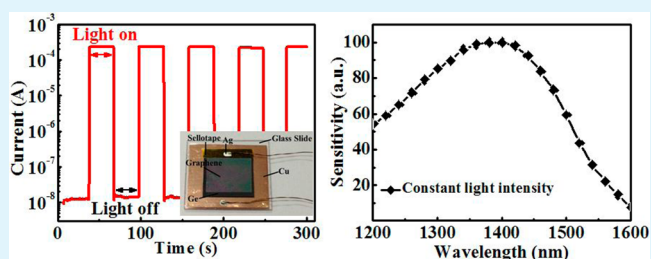
Long-Hui Zeng,<sup>†</sup> Ming-Zheng Wang,<sup>†</sup> Han Hu,<sup>†</sup> Biao Nie,<sup>†</sup> Yong-Qiang Yu,<sup>†</sup> Chun-Yan Wu,<sup>†</sup> Li Wang,<sup>†</sup> Ji-Gang Hu,<sup>†</sup> Chao Xie,<sup>†,‡</sup> Feng-Xia Liang,<sup>\*,‡</sup> and Lin-Bao Luo<sup>\*,†</sup>

<sup>†</sup>School of Electronic Science and Applied Physics and Anhui Provincial Key Laboratory of Advanced Functional Materials and Devices, and <sup>‡</sup>School of Materials Science and Engineering, Hefei University of Technology, Hefei, Anhui 230009, P. R. China

## Supporting Information

**ABSTRACT:** We report on the simple fabrication of monolayer graphene (MLG)/germanium (Ge) heterojunction for infrared (IR) light sensing. It is found that the as-fabricated Schottky junction detector exhibits obvious photovoltaic characteristics, and is sensitive to IR light with high  $I_{\text{light}}/I_{\text{dark}}$  ratio of  $2 \times 10^4$  at zero bias voltage. The responsivity and detectivity are as high as  $51.8 \text{ mA W}^{-1}$  and  $1.38 \times 10^{10} \text{ cm Hz}^{1/2} \text{ W}^{-1}$ , respectively. Further photoresponse study reveals that the photovoltaic IR detector displays excellent spectral selectivity with peak sensitivity at 1400 nm, and a fast light response speed of microsecond rise/fall time with good reproducibility and long-term stability. The generality of the above results suggests that the present MLG/Ge IR photodetector would have great potential for future optoelectronic device applications.

**KEYWORDS:** Schottky junction, infrared photodetector, heterojunction, photovoltaic effect, response speed



## INTRODUCTION

Infrared (IR) photodetector, as a type of widely studied device of great practical importance, is a crucial component for wide-ranging applications in many areas such as military surveillance, target detection, and target tracking. To date, numerous IR photodetectors have been developed from narrow band gap semiconductors such as PbS, InSb, CdZnTe, HgCdTe, etc.<sup>1</sup> In addition, germanium (Ge) as an important semiconductor material of IV group,<sup>2,3</sup> can be employed to fabricate infrared (IR) photodetectors as well. Because of the distinct property including large absorption coefficient at near-infrared frequencies, low cost, and excellent compatibility of parallel processing with silicon technology, great efforts have been devoted to fabricating on-chip Ge photodetectors with exceptionally high speed and responsivity.<sup>4</sup> So far, a number of Ge-based IR photodetectors with different device configurations have been developed, including metal-semiconductor-metal,<sup>5,6</sup> p-i-n,<sup>7,8</sup> semiconductor/metal Schottky junction photodetectors,<sup>4</sup> Ge/Si junction.<sup>9</sup> In spite of these research efforts, it is undeniable that the fabrication of these devices normally requires very complicated instruments, which leads to high costs and energy consumption, and therefore constitutes the main obstacle to their wide application.

A possible solution to the above predicament is to design graphene/semiconductor Schottky-type IR photodetectors featuring low dark current, high response speed, and small parasitic capacitance. Graphene, as a promising material for transparent electrode, has extraordinary properties such as high optical transmittance, larger thermal conductivity, excellent

electronic and mechanical properties, as well as outstanding chemical/physical stability with tunable work function.<sup>10,11</sup> Owing to these fascinating electrical and optical properties, graphene has been successfully combined with other semiconductor materials such as ZnO, CdSe for high-performance ultraviolet (UV), and visible light photodetectors application.<sup>12,13</sup> Enlightened by this, we propose a simple IR detector that combines monolayer graphene (MLG) with bulk Ge wafer that will possibly provide synergistic effects in light absorption and electron transport, and therefore will bring about improved device performance. It is found that the Schottky junction diode is highly sensitive to IR light irradiation at zero bias voltage with good reproducibility. The responsivity, detectivity, and response time are estimated to be  $51.8 \text{ mA W}^{-1}$ ,  $1.38 \times 10^{10} \text{ cm Hz}^{1/2} \text{ W}^{-1}$ , and  $23 \mu\text{s}$ , respectively. What is more, the IR sensor exhibits excellent spectral selectivity with peak sensitivity at 1400 nm. The generality of the above result suggests that this MLG/Ge IR detector will have potential application in future optoelectronics devices.

## RESULTS AND DISCUSSION

To fabricate the photovoltaic IR photodetector, we etched 400  $\mu\text{m}$  thick n-type Ge wafer with resistivity of 0.1–0.4  $\Omega \text{ cm}$  by using HF buffer etching (BOE) solution to remove thin  $\text{GeO}_2$  layer on the surface. Then sellotape was stuck at the periphery

Received: July 4, 2013

Accepted: September 16, 2013

Published: September 16, 2013

of the cleaned Ge wafer ( $1 \times 1 \text{ cm}^2$ ) for insulation purpose. The MLG films were grown at  $1000 \text{ }^\circ\text{C}$  by using a mixed gas of  $\text{CH}_4$  (40 sccm) and  $\text{H}_2$  (20 sccm) via a CVD method in which  $25 \text{ }\mu\text{m}$  thick Cu foils were employed as the catalytic substrates. After growth, the graphene films were spin-coated with 5 wt % polymethylmethacrylate (PMMA) in chlorobenzene, and then the underlying Cu foil were removed in Marble's reagent solution ( $\text{CuSO}_4 \cdot \text{HCl} \cdot \text{H}_2\text{O} = 10 \text{ g}:50 \text{ mL}:50 \text{ mL}$ ). The graphene films were rinsed in deionized water to remove the remaining ions.<sup>14</sup> Afterward, the as-treated Ge wafer was soaked in deionized water, and then slowly lifted to mount the MLG films on the Ge. The as-assembled device was eventually transferred onto a copper foil, on which silver paste was coated to form good contact between the Ge and the underlying copper. The microstructure of the MLG was characterized by Raman spectrum. Figure 1a shows a typical Raman spectrum

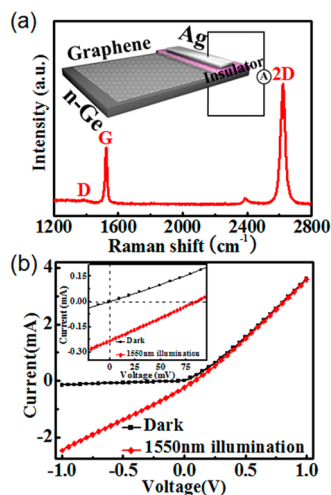


**Figure 1.** (a) Raman spectrum of the monolayer graphene film, the inset is the schematic illustration of the MLG/Ge photovoltaic IR photodetector. (b)  $I$ – $V$  characteristics of the IR photodetector measured at room temperature with and without IR irradiation, the inset shows the magnified  $I$ – $V$  characteristics of MLG/Ge Schottky junction in low voltage range.

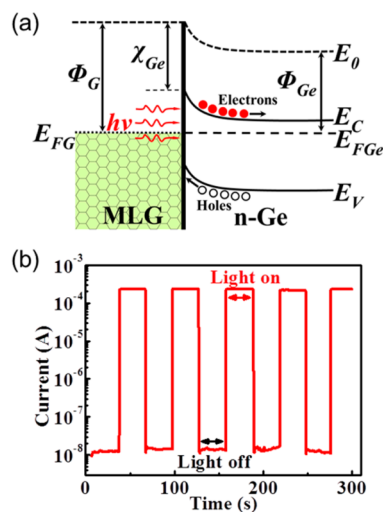
which is composed of two sharp peaks, i.e., 2D band peak at  $\sim 2623 \text{ cm}^{-1}$  and G band peak at  $\sim 1525 \text{ cm}^{-1}$ . The intensity ratio of  $I_{2D}:I_G \approx 2.1$ , along with the weak D band scattering at  $\sim 1343 \text{ cm}^{-1}$ , confirms the high crystal quality of the monolayer graphene film.<sup>15,16</sup> In this study, the MLG mainly functions as a transparent electrode. Namely, it can not only allow the majority of the incident light to reach the contact area but also transport carriers when the electron–holes were separated. On the other hand, the flat and bulk Ge substrate will provide sufficient contact area for the MLG, which is vitally important for the formation of effective Schottky junction. The electrical characteristic of the MLG/Ge Schottky junction was evaluated by an  $I$ – $V$  characterization system (Keithley 4200 SCS). The photoresponse of the IR photodetectors was studied by using a 1550 nm laser (DFB light source, China-fiber) as light source. To determine the spectral response and time response of the IR photodetectors, we used a home-built system composed of a light source (LE-SP-LS-XE), a monochromator (LE-SP-M300), an oscilloscope (Tektronix, TDS2012B), and an optical chopper (LE-oc120).

Figure 1b shows the current–voltage ( $I$ – $V$ ) curves of a typical heterojunction at room temperature, from which one

can see that the device exhibits typical rectifying behavior. The nearly linear  $I$ – $V$  curves of both Ag/MLG and Ge/Ag/Cu (see Figure S1 in the Supporting Information) signify that such a rectifying characteristic arises from Schottky barrier of Ge/MLG, which can be described by the thermionic-emission based diode equation<sup>17</sup>

$$J(T, V) = J_s(T) \left[ \exp\left(\frac{eV}{\eta k_B T}\right) - 1 \right] \quad (1)$$

where  $J(T, V)$  is the current density across the MLG/Ge interface,  $V$  the applied voltage,  $k_B$  the Boltzmann's constant,  $T$  the absolute temperature,  $\eta$  the ideality factor ( $\eta = (q/kT)(dV/d \ln I)$ ). The prefactor,  $J_s(T)$  is the saturation current density and can be expressed by  $J_s(T) = A^* T^2 \exp(-e\phi_{\text{SBH}}/k_B T)$ ,<sup>17</sup> whereas the zero bias Schottky barrier height (SBH),  $A^*$  the Richardson constant,  $m^*$  the effective mass of the charge carriers. For Ge,  $A^*$  is theoretically estimated to be  $66 \text{ A cm}^{-2} \text{ K}^{-2}$  ( $m_e^* = 0.55m_0$ ).<sup>12</sup> Using the  $J_s$  value, the Schottky barrier height at the MLG/Ge interface was estimated to be 0.455 V. This barrier height is comparable to that of graphene/n-type silicon (0.41 V).<sup>18</sup> Interestingly, when exposed to 1550 nm IR irradiation, the Schottky barrier of MLG/Ge, like ZnO/Au Schottky junction,<sup>19</sup> almost disappeared, giving way to a huge photocurrent at reverse bias. This remarkable photocurrent is associated with photoexcited carriers under IR light illumination. Careful examination of the  $I$ – $V$  curves found that the device exhibits typical photovoltaic effect (c.f. the inset of Figure 1b), with an open-circuit voltage ( $V_{\text{OC}}$ ), a short-circuit current ( $I_{\text{SC}}$ ) and a fill factor ( $FF$ ) of 0.085 V, 0.23 mA, and 0.25, respectively, yielding a PCE of 0.11%. Comparison of the Ag/MLG or Ge/Ag(silver paste)/Cu found that such a photovoltaic effect is due to the MLG/Ge Schottky junction, rather than Ag/MLG or Ge/Ag(silver paste)/Cu (as shown in Figure S1 in the Supporting Information). This photovoltaic characteristic can be understood from the energy band diagram illustrated in Figure 2a. Once the MLG was transferred onto Ge wafer, electrons in Ge tend to move to the graphene side and



**Figure 2.** (a) Energy band diagram of the IR photodetector under IR illumination.  $\chi_{\text{Ge}}$  is the electron affinity of Ge.  $\Phi_G/\Phi_{\text{Ge}}$  and  $E_{\text{FG}}/E_{\text{FGe}}$  denote the work functions and Fermi energy levels of MLG/Ge, respectively;  $E_C$  and  $E_V$  are the conduction and valence bands of Ge, respectively. (b) Photoreponse of the device under 1550 nm light illumination without external bias voltage.

consequently the energy levels near the Ge surface will bend upward, leading to the formation of built-in electric field near the MLG/Ge interface. Under light illumination, photo-generated electron–hole pairs will be separated by the built-in electric field. The resulted free electrons and holes will move toward opposite directions, giving rise to generation of photovoltaic current in external circuit. The photovoltage is formed as a result of the energy difference between the Fermi level of Ge and the MLG under illumination. Although the generation of photocurrent in the MLG/Ge is inefficient in comparison with MLG/Si,<sup>20</sup> the weak photovoltaic effect can enable the Schottky junction to sense IR illumination without external energy supply. Figure 2b displays the representative photoresponse of an IR sensor when light was turned on and off alternately at zero bias voltage. It demonstrates clearly that our device can be reversibly switched between low- and high-resistivity states, with a high  $I_{\text{light}}/I_{\text{dark}}$  ratio of  $2 \times 10^4$ . The steep rise and fall edges suggest the swift response speed.

To further reveal the response properties of the IR sensor, we investigated the bias voltage dependent photoresponse of the IR detector. Figure 3a shows a family of  $I$ – $V$  curves under

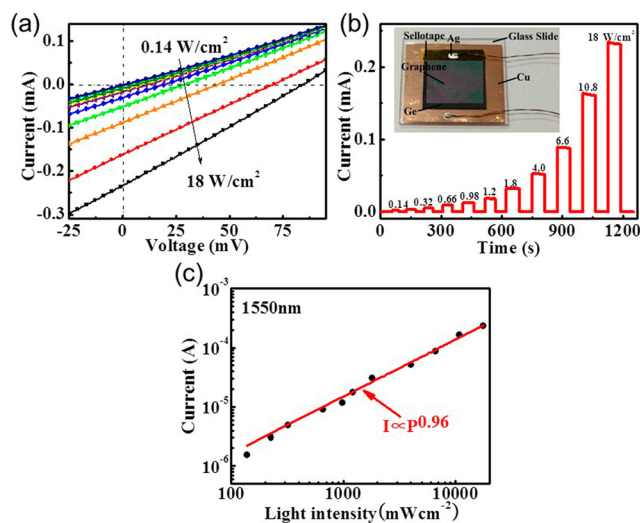


**Figure 3.** (a) Photovoltaic characteristics of the MLG/Ge device when the incident light power was gradually increased from 0.14 to 18 W/cm<sup>2</sup>. (b) Corresponding photoresponse of the IR detector; the inset shows a digital photograph of the IR photodetector. (c) Fitting curve of the relationship between the photocurrent and light intensity; the light wavelength was 1550 nm.

increasing incident light intensity (from  $P = 0.14$  to 18 W/cm<sup>2</sup>), from which one can see that the photocurrent of the device is highly dependent on the bias voltage. Further experimental result reveals that both on and off currents will monotonously increase when the bias voltage was decreased from  $-0.2$  to  $-1.0$  V. In addition, the corresponding responsivity is observed to increase with increasing voltage (see Figure S2 in the Supporting Information). Figure 3b displays the photocurrent under IR light irradiation with different intensities. Basically, the photocurrent of the device increases gradually with increasing radiation power. This dependence of photocurrent on light intensity can be fitted by a simple power law:  $I = AP^\theta$ , where  $A$  is a constant for a certain wavelength, and the exponent determines the response of photocurrent to light intensity.<sup>21</sup> Fitting the curve leads to  $\theta = 0.96$ , in other words, the photocurrent is nearly proportional

to the incident light intensity.<sup>22</sup> This nearly integer exponent suggests that there is little trap states in our photodetector.<sup>23,24</sup>

It should be noted that the present MLG/Ge IR detector exhibits excellent reproducibility as well. Figure 4a shows the

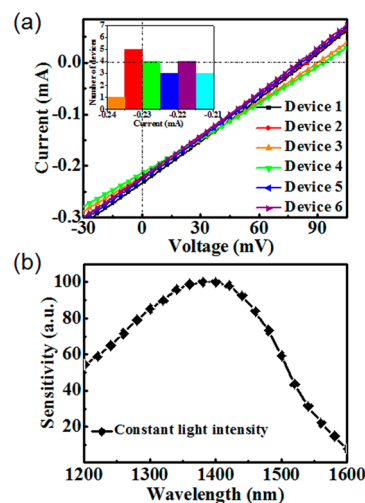


**Figure 4.** (a) Photovoltaic characteristics of 6 representative devices under IR light illumination, inset shows the distributional histogram of the photocurrent for 20 devices. (b) Spectral response of a representative IR photodetector.

$I$ – $V$  curve of 6 representative devices, from which one can see that all the curves virtually overlap. Further photocurrent histogram of 20 devices reveals that the majority of photocurrent is in the range from  $-0.215$  to  $-0.235$  mA (see the inset of Figure 4a), with an average value of 0.225 mA. This reliable characteristic is vitally important and will enable the MLG/Ge Schottky junction to function as commercial device. To quantify the performance of such an IR photodetector, other two key metrics including responsivity ( $R$ ) and detectivity ( $D^*$ ) that reflect the photodetector sensitivity to incident light were calculated by using the following equations

$$R(AW^{-1}) = \frac{I_p}{P_{\text{opt}}} = \eta \left( \frac{q\lambda}{hc} \right) G \quad (2)$$

$$D^* = A^{1/2} R / (2qI_d)^{1/2} = A^{1/2} (I_p / P_{\text{opt}}) / (2qI_d)^{1/2} \quad (3)$$

where  $I_p$ ,  $P_{\text{opt}}$ ,  $\eta$ ,  $h$ ,  $c$ ,  $\lambda$ ,  $A$ ,  $q$ ,  $I_d$ , and  $G$  are photocurrent, incident light power, quantum efficiency, Planck constant, speed of light, light wavelength, active area, the unit of elementary charge, dark current, and photoconductive gain, respectively. The responsivity ( $R$ ) is estimated to be 51.8 mA W<sup>-1</sup> at zero bias (assuming  $\eta = 1$  for simplification). This  $R$ , much higher than that of the conventional Si photodetector,<sup>25</sup> is dependent on the biasing voltage applied on the device (see Figure S2 in the Supporting Information). On the basis of above values and the active area of 0.025 mm<sup>2</sup> (the spot area of the laser), the detectivity ( $D^*$ ) is estimated to be  $1.38 \times 10^{10}$  cm Hz<sup>1/2</sup> W<sup>-1</sup>, which is comparable with that of bulk Si based photodetector.<sup>26</sup> Apart from the high responsivity and detectivity, the MLG/Ge IR detector exhibits good spectral selectivity. Figure 4b) plots the normalized responsivity of the IR detector as a function of wavelength (to make the analysis more reliable, we kept the light power identical for all wavelengths during testing). It can be seen that the present device exhibits peak sensitivity at 1400 nm, corresponding

closely to the intrinsic absorption of Ge crystal. This consistency is believed to be highly related to the working mechanism, which has been studied in our previous work.<sup>21</sup> This excellent spectral selectivity, along with the low cost and simple fabrication process, will make the present device highly practical in future IR detection.

Next, the response speed of the device is examined. Figure 5a shows the time response when exposed to the pulsed IR light

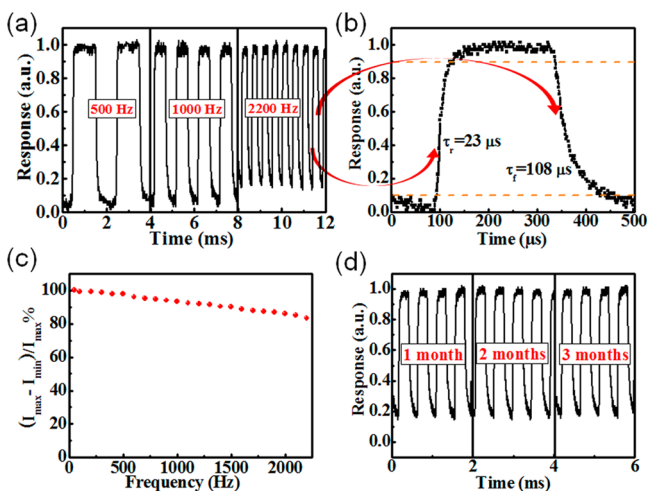


**Figure 5.** (a) Photoreponse of the photovoltaic detector to pulsed IR light irradiation (1550 nm laser) with a frequency of 500, 1000, and 2200 Hz. (b) A single normalized cycle measured at 2200 Hz for estimating both response time ( $\tau_r$ ) and recovery time ( $\tau_f$ ). (c) The relative balance  $(I_{\max} - I_{\min})/I_{\max}$  versus switching frequency. (d) Photoreponse behavior of the IR detector after long-term storage.

(1550 nm). For all switching frequencies, the response is fast and exhibits long-term repeatability in the frequency range from 0 to 2200 Hz. Notably, even at 2200 Hz, the relative balance only decreases by less than 18%. Namely, this IR detector is able to monitor pulsed optical signal with very high frequency.<sup>24</sup> In the time domain, the response speed of the IR photodetector is normally assessed by the response time ( $\tau_r$ ), which is the time interval for the response to rise from 10 to 90% of its peak value. The recovery time ( $\tau_f$ ) is the time interval for the response to decay from 90 to 10% of its peak value.<sup>13,24,27</sup> Specifically, when the device is working under a pulsed light with the switching frequency of 2200 Hz, a small response/recovery time ( $\tau_r/\tau_f$ ) of 23/108  $\mu\text{s}$  was obtained. This response speed is slower than the commercial germanium photodetector (Table 1), but much quicker than other graphene based photodetectors, including CdSe nanobelt/graphene heterojunction, and ZnO nanowires/graphene heterojunction.<sup>28,29</sup> We attribute this relatively quick response speed to the extremely high carrier mobility due to high crystallinity with a low density of trap centers, and quick separation of huge amount of photogenerated carriers by the built-in electric field formed at the MLG/Ge interface. Finally, it should be noted that, unlike the majority of IR devices based on nanostructures, the present MLG/Ge Schottky junction can work properly even after long-term storage. As shown in Figure 5d, our device can retain the same photocurrent after 3 months storage in drying box.

**Table 1. Summary of the Device Performances of the MLG/Ge Photovoltaic IR Detector and Other Photodetectors with Similar Device Structures**

device structure	responsivity	rise time ( $\tau_r$ )	fall time ( $\tau_f$ )	$I_{\text{light}}/I_{\text{dark}}$	ref
graphene/Ge Schottky junction	51.8 mA/W	23 $\mu\text{s}$	108 $\mu\text{s}$	$\sim 1 \times 10^4$	our work
graphene/ZnO nanorod array Schottky junction	113 A/W	0.7 ms	3.6 ms		12
CdSe nanobelt/graphene Schottky junction on PET	8.7 A/W	70 $\mu\text{s}$	137 $\mu\text{s}$	$\sim 1 \times 10^5$	13
CdSe nanobelt/graphene Schottky junction on SiO <sub>2</sub> /Si	10.2 A/W	82 $\mu\text{s}$	179 $\mu\text{s}$	$\sim 1 \times 10^5$	16
graphene/Si heterojunction	0.2 A/W	1.2 ms	3 ms	$\sim 1 \times 10^4$	26
MWNT/n-Si heterojunction	100 $\mu\text{A/W}$	16 ms	16 ms		25
p-CdTe NR/n-SiNWs heterojunction		1.2 ms	1.58 ms	$\sim 1 \times 10^5$	28
p-ZnS NR/n-Si heterojunction	200 A/W	48 $\mu\text{s}$	180 $\mu\text{s}$	36	29
metal-Ge-metal	0.24 A/W	2 ns			5

## CONCLUSION

In conclusion, we demonstrated the fabrication of a high-performance photovoltaic type IR photodetector based on the MLG/Ge Schottky junction. Electrical analysis reveals that the as-fabricated device was highly sensitive to IR irradiation with peak sensitivity at 1400 nm, good reproducibility, excellent spectral selectivity and long-term stability. The  $I_{\text{light}}/I_{\text{dark}}$  ratio, responsivity and detectivity of the device were estimated to be  $2 \times 10^4$ , 51.8 mA/W, and  $1.38 \times 10^{10}$  cm Hz<sup>1/2</sup> W<sup>-1</sup>, respectively. What is more, the response speed is as quick as 23  $\mu\text{s}$ , much quicker than other conventional photodetectors. It is expected that this simple, but high-performance MLG/Ge device will have potential application for future IR detection.

## ASSOCIATED CONTENT

### Supporting Information

Electrical property of both Ag/MLG and Ge/Ag/Cu contacts, bias voltage dependent photoresponse behavior, the  $I_{\text{light}}/I_{\text{dark}}$  and responsivity at varied bias voltages. This material is available free of charge via the Internet at <http://pubs.acs.org>.

## AUTHOR INFORMATION

### Corresponding Authors

\*E-mail: [fxliang@hfut.edu.cn](mailto:fxliang@hfut.edu.cn).

\*E-mail: [luolb@hfut.edu.cn](mailto:luolb@hfut.edu.cn).

### Notes

The authors declare no competing financial interest.

## ACKNOWLEDGMENTS

This work was supported by the National Natural Science Foundation of China (NSFC, 51172151, 21101051), the Fundamental Research Funds for the Central Universities (2011HGZJ0004, 2012HGCX0003, 2013HGCH0012), the China Postdoctoral Science Foundation (103471013).

## REFERENCES

- Rogalski, A. *Infrared Phys. Technol.* **2002**, *43*, 187–210.
- Assefa, S.; Xia, F. N.; Vlasov, Y. A. *Nature* **2010**, *464*, 80–84.

- (3) Tang, L.; Kocabas, S. E.; Latif, S.; Okyay, A. K.; LyGagnon, D. S.; Saraswat, K. C.; Miller, D. A. *Nat. Photonics* **2008**, *2*, 226–229.
- (4) Cao, L. Y.; Park, J. S.; Fan, P. Y.; Clemens, B.; Brongersma, M. L. *Nano Lett.* **2010**, *10*, 1229–1233.
- (5) Colace, L.; Masini, G.; Galluzzi, F.; Assanto, G.; Capellini, G.; Di Gaspare, L.; Palange, E.; Evangelisti, F. *Appl. Phys. Lett.* **1998**, *72*, 3175–3177.
- (6) Yan, C. Y.; Singh, N.; Cai, H.; Gan, C. L.; Lee, P. S. *ACS Appl. Mater. Interfaces* **2010**, *2*, 1794–1797.
- (7) Vivien, L.; Osmond, J.; Fédéli, J. M.; Marriss Morini, D.; Crozat, P.; Damlencourt, J. F.; Cassan, E.; Lecunff, Y.; Laval, S. *Opt. Express* **2009**, *17*, 6252–6257.
- (8) Feng, D. Z.; Liao, S. R.; Dong, P.; Feng, N. N.; Liang, H.; Zheng, D. W.; Kung, C. C.; Fong, J.; Shafiha, R.; Cunningham, J. *Appl. Phys. Lett.* **2009**, *95*, 261105.
- (9) Sahni, S.; Luo, X.; Liu, J.; Xie, Y. H.; Yablonovitch, E. *Opt. Lett.* **2008**, *33*, 1138–1140.
- (10) Kim, K. S.; Zhao, Y.; Jang, H.; Lee, S. Y.; Kim, J. M.; Kim, K. S.; Ahn, J. H.; Kim, P.; Choi, J. Y.; Hong, B. H. *Nature* **2009**, *457*, 706–710.
- (11) Lee, C. G.; Wei, X. D.; Kysar, J. W.; Hone, J. *Science* **2008**, *321*, 385–388.
- (12) Nie, B.; Hu, J. G.; Luo, L. B.; Xie, C.; Zeng, L. H.; Lv, P.; Li, F. Z.; Jie, J. S.; Feng, M.; Wu, C. Y.; Yu, Y. Q.; Yu, S. H. *Small* **2013**, *9*, 2872–2879.
- (13) Gao, Z. W.; Jin, W. F.; Zhou, Y.; Dai, Y.; Yu, B.; Liu, C.; Xu, W. J.; Li, Y. P.; Peng, H. L.; Liu, Z. F.; Dai, L. *Nanoscale* **2013**, *5*, 5576–5581.
- (14) Xie, C.; Jie, J. S.; Nie, B.; Yan, T. X.; Li, Q.; Lv, P.; Li, F. Z.; Wang, M. Z.; Wu, C. Y.; Wang, L.; Luo, L. B. *Appl. Phys. Lett.* **2012**, *100*, 193103.
- (15) Xie, C.; Lv, P.; Nie, B.; Jie, J. S.; Zhang, X. W.; Wang, Z.; Jiang, P.; Hu, Z. Z.; Luo, L. B.; Zhu, Z. F.; Wang, L.; Wu, C. Y. *Appl. Phys. Lett.* **2011**, *99*, 133113.
- (16) Jin, W. F.; Ye, Y.; Gan, L.; Yu, B.; Wu, P. C.; Dai, Y.; Meng, H.; Guo, X. F.; Dai, L. *J. Mater. Chem.* **2012**, *22*, 2863–2867.
- (17) Miao, X. C.; Tongay, S.; Petterson, M. K.; Berke, K.; Rinzler, A. G.; Appleton, B. R.; Hebard, A. F. *Nano Lett.* **2012**, *12*, 2745–2750.
- (18) Chen, C. C.; Aykol, M.; Chang, C. C.; Levi, A. F. J.; Cronin, S. B. *Nano Lett.* **2011**, *11*, 1863–1867.
- (19) Keem, K.; Kim, H.; Kim, G. T.; Lee, J. S.; Min, B.; Cho, K.; Sung, M. Y.; Kim, S. *Appl. Phys. Lett.* **2004**, *84*, 4376–4378.
- (20) Xie, C.; Zhang, X. Z.; Wu, Y. M.; Zhang, X. J.; Zhang, X. W.; Wang, Y.; Zhang, W. J.; Gao, P.; Han, Y. Y.; Jie, J. S. *J. Mater. Chem. A* **2013**, *1*, 8567–8574.
- (21) Wang, M. Z.; Liang, F. X.; Nie, B.; Zeng, L. H.; Zheng, L. X.; Lv, P.; Yu, Y. Q.; Xie, C.; Li, Y. Y.; Luo, L. B. *Part. Part. Syst. Charact.* **2013**, *30*, 630–636.
- (22) Kung, S. C.; van der Veer, W. E.; Yang, F.; Donovan, K. C.; Penner, R. M. *Nano Lett.* **2010**, *10*, 1481–1485.
- (23) Kind, H.; Yan, H. Q.; Messer, B.; Law, M.; Yang, P. D. *Adv. Mater.* **2002**, *14*, 158–160.
- (24) Wu, D.; Jiang, Y.; Zhang, Y. G.; Li, J. W.; Yu, Y. Q.; Zhang, Y. P.; Zhu, Z. F.; Wang, L.; Wu, C. Y.; Luo, L. B.; Jie, J. S. *J. Mater. Chem.* **2012**, *22*, 6206–6212.
- (25) Ong, P. L.; Euler, W. B.; Levitsky, I. A. *Appl. Phys. Lett.* **2010**, *96*, 033106.
- (26) An, X. H.; Liu, F. Z.; Jung, Y. J.; Kar, S. *Nano Lett.* **2013**, *13*, 909–916.
- (27) Wu, P. C.; Dai, Y.; Sun, T.; Ye, Y.; Meng, H.; Fang, X. L.; Yu, B.; Dai, L. *ACS Appl. Mater. Interfaces* **2011**, *3*, 1859–1864.
- (28) Xie, C.; Luo, L. B.; Zeng, L. H.; Zhu, L.; Chen, J. J.; Nie, B.; Hu, J. G.; Li, Q.; Wu, C. Y.; Wang, L.; Jie, J. S. *CrystEngComm* **2012**, *14*, 7222–7228.
- (29) Yu, Y. Q.; Luo, L. B.; Zhu, Z. F.; Nie, B.; Zhang, Y. G.; Zeng, L. H.; Zhang, Y.; Wu, C. Y.; Wang, L.; Jiang, Y. *CrystEngComm* **2013**, *15*, 1635–1642.